PARAMETER ESTIMATION AND ANALYSIS OF ACTUATORS FOR THE BACT WIND-TUNNEL MODEL

Martin R. Waszak* and Jimmy Fung,† *NASA Langley Research Center, Hampton, Virginia*

Abstract

This paper describes the development of transfer function models for the trailing edge and upper- and lower-spoiler actuators of the Benchmark Active Control Technology (BACT) wind-tunnel model for application to control system analysis and design. A simple nonlinear least squares parameter estimation approach is applied to determine transfer function parameters from frequency response data. Unconstrained quasi-Newton minimization of weighted frequency response error was employed to estimate the transfer function parameters. An analysis of the behavior of the actuators over time to assess the effects of wear and aerodynamic load using the transfer function models is also presented. The frequency responses indicate consistent actuator behavior throughout the wind-tunnel test and only slight degradation in effectiveness due to aerodynamic hinge loading. The resulting actuator models have been used in design, analysis, and simulation of controllers for the BACT. The resulting controllers have successfully suppressed flutter over a wide range of conditions.

Introduction

The ability of an active control system to accomplish the function for which it was designed depends to a large degree on the accuracy of the mathematical models used to describe the dynamic behavior of the physical system to be controlled. A crucial element of the overall system is the actuator. The commanded control inputs need to be accurately produced by the actuators in order to achieve the desired level of performance. Mathematical models that characterize the dynamic response of the actuators are therefore key requirements for design, analysis, and simulation of any control system.

The objective of this paper is to develop a set of actuator models for the Benchmark Active Control Technology (BACT) wind-tunnel model[1,2] that is appropriate for application to control system analysis and design. This type of application does not require the actuator model structure and parameter estimates to be particularly accurate, however, the dynamic input-output properties of the actuators over the frequency range of interest for the BACT wind-tunnel model should be fairly accurate.

Control system design usually takes into account design model variations and uncertainty in the form of gain and phase margins. Typical gain and phase margins might be ±6 dB and ±30 degrees, respectively. Errors in the actuator models should only represent a small fraction of these margins -- perhaps 10 percent or so. Input-output frequency response accuracy will be the basis for the acceptability of the actuator model structure and parameter estimates and will be measured in terms of magnitude and phase compared to experimental frequency response data. The accuracy of the parameter estimates themselves will not be considered.

Development of the actuator models begins by an assessment of the physical systems of the BACT wind-tunnel model and a review of the available data. An actuator model structure is then chosen based on the physical characteristics of hydraulic systems. A simple parameter estimation procedure based on minimizing weighted frequency response error using a quasi-Newton scheme is outlined. The parameters of the model structure are determined from experimental frequency response data and analyzed to assess variations in the actuator dynamic input-output characteristics over time (due to servo loop gain variations and bearing, seal, and sensor wear) and the effects of control surface hinge loading due to aerodynamics.

Note that frequency response data will be treated as the truth data for the parameter estimation process. The frequency response data is based, however, on *estimates* of the power spectra of actuator responses obtained from experimental data using fast Fourier transform (FFT) techniques. As a result, the frequency response data has estimation errors associated with it that depend on the way in which the time histories were recorded and the manner in which the FFT's were

* Aerospace Research Engineer, Senior Member AIAA.

† Cooperative Education Student, Virginia Polytechnic and State University, Student Member AIAA.

computed.[3] The errors introduced by the FFT process will not be considered here.

Experimental Setup

The Benchmark Active Controls Technology (BACT) project is part of NASA Langley Research Center's Benchmark Models Program[4] for studying transonic aeroelastic phenomena. The BACT system was developed to collect high quality unsteady aerodynamic data (pressures and loads) near transonic flutter conditions and demonstrate flutter suppression. Figure 1 depicts an illustration of the BACT wind-tunnel experimental setup.

The BACT system consists of a rigid wing section and a flexible mounting system. [5,6] The wind-tunnel model is a rigid, rectangular wing with an NACA 0012 airfoil section. It is equipped with a trailing-edge control surface, and upper- and lower-surface spoilers that are controlled independently by hydraulic actuators. It is instrumented with pressure transducers, accelerometers, actuator position sensors, and hydraulic pressure transducers. The wing is mounted to a device called the Pitch and Plunge Apparatus (or PAPA) which is designed to permit motion in principally two modes -- rotation (or pitch), and vertical translation (or plunge). The BACT system was precisely tuned to flutter within the operating range of the Transonic Dynamics Tunnel (TDT)[7] at NASA Langley Research Center in which the system was tested.

The actuators in the trailing edge and upper- and lower-spoiler control surface assemblies were specifically designed for the BACT wind-tunnel model because of the space limitations arising from placing the two spoilers and trailing edge control surface within close proximity of each other. The trailing edge control surface is driven by a rotary vane actuator and the spoilers are driven by piston actuators.[8] Each

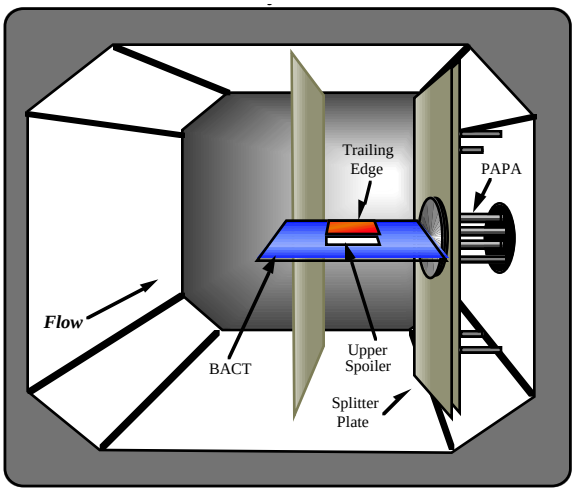

Figure 1 - BACT wind-tunnel test setup.

actuator has a servo-loop as depicted in the block diagram in Figure 2. The control surface position sensors and hydraulic pressure transducers were used as servo feedback signals. The gains on position error, $\delta_c - \delta$, and differential hydraulic pressure, Δhp, could be adjusted to alter the response characteristics of the actuator.

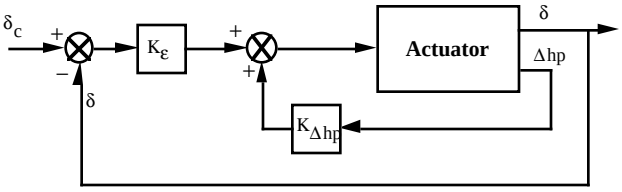

Figure 2 - Servo Loop for BACT Actuators.

Experimental Data

A large set of experimental frequency response data for the BACT actuators was available from a wind-tunnel test. The data was not generated with parameter estimation in mind and consequently was not ideal for parameter estimation applications. However, it provides a basis upon which actuator models with sufficient accuracy for control system design applications can be obtained.

The actuator data was collected during an experiment that took place early in 1995. The test lasted approximately four weeks during which over 2300 test points were recorded. The average duration of each test point was about five minutes. About half of the test points involved some level of actuator activity. Roughly three quarters of the test points involving control activity used the trailing edge control and the other quarter used the upper-spoiler. The lower-spoiler was used very little during the test.

Excitation of the control surfaces for actuator performance assessments was performed periodically throughout the test at a variety of Mach numbers and dynamic pressure conditions. The excitations were performed under open-loop conditions, that is, there was no feedback around the BACT system. Commanded excitations, either linear sine sweeps or random sequences, had a duration of either 25 or 75 seconds. Control surface commands and the resulting control surface position signals were recorded at a rate of 200 samples per second.

The time response data was converted into frequency response form. Fast Fourier transform (FFT) techniques were used to compute estimates of the cross- and auto- spectral density of actuator command and control surface position. The frequency response of the actuator was then determined taking the ratio of the appropriate cross- and auto-spectra. The FFT's were computed using the method described in

Reference 9 and used a Hanning window, 2K data blocks, and 75% overlap averaging. The frequency response data are the basis for the actuator modeling that will be described subsequently.

Since data was available at various points throughout the test it is possible to assess variations in the actuator dynamic characteristics. As the test progressed several factors could have influenced the actuator dynamics. The position error gain of the actuator servo loops was altered at various times during the test to maintain desired response characteristics and to attempt to eliminate chatter that appeared in some control surface responses. The differential hydraulic pressure gain was zero throughout the test. The change in the position error gain was not measured or recorded and so represents an unknown variation. In addition, the use of the actuators led to wear in the seals, bearings, and position sensor potentiometers that could have altered the actuator responses.

In order to establish a reference for chronological comparison as a basis for the assessment of variations over time, three data sets were chosen to represent data acquired early, in the middle, and late in the test. These data sets will be referred to in this paper as 'Early,' 'Middle,' and 'Late,' respectively, and roughly correspond to data collected during the first, second, and third weeks of the test. The number of cycles that each actuator completed throughout the test varied considerably. Therefore, the potential for variations over time was different for each actuator.

The effect of aerodynamic loading on the actuator characteristics could also be assessed since data was available at a variety of operating conditions (Mach numbers and dynamic pressures). The experimental data was qualitatively categorized by aerodynamic loading condition, either loaded or unloaded. The loaded condition is therefore representative of a relatively wide range of Mach numbers and dynamic pressures and represents a general basis upon which the effect of control surface hinge loads can be assessed. Comparing frequency responses for the actuator with and without aerodynamic loading gives an indication of the degree to which the actuator behavior could vary over the range of operating conditions.

Actuator Model Structure

The mathematical models for the BACT actuators were based on a third order transfer function structure that characterizes the key features of hydraulic systems.[10,11]

$$\frac{\delta(s)}{\delta_c(s)} = \frac{k p \omega^2}{(s+p)(s^2 + 2\zeta\omega s + \omega^2)} \qquad (1)$$

where δ is the angular position of the control surface and δ_c is the actuator command. There are four unknown parameters in this transfer function structure: k is a gain, p is a first order pole, and ω and ζ are second order frequency and damping. The first order pole is associated with the flow of hydraulic fluid through a small orifice and the gain on control surface position error feedback. The second order frequency and damping are associated with the compressibility of the hydraulic fluid, the inertia of the control surface, the compliance of the structure, and the gain on control surface position error.

The transfer function approach to modeling the actuator is able to characterize the key dynamics of the hydraulic actuators of major interest in control system design. It cannot, however, characterize nonlinearities such amplitude dependent gains, dead zone and backlash, or position and rate limits. These effects must be addressed by other means.

A transfer function model structure was selected because of its inherently simple structure and the ease with which it can be integrated into control system analysis, design, and simulation.

Parameter Estimation

The four transfer function parameters from Eqn (1) were estimated from experimental frequency response data using the process described by the flowchart shown in Figure 3. The process involves defining a cost (or error) function and minimizing that function by the selection of the desired parameter set, (k,p,ω,ζ). First, an initial parameter set was selected and the resulting analytical frequency response data, in magnitude and phase form, was computed at the same frequencies for which the experimental data was available. The magnitude and phase errors between the analytical and experimental data were then calculated. A weighted sum square of the transfer function magnitude and phase errors, ε^2, was minimized within an optimization routine. The frequency response based on the parameters resulting from the optimization were then compared to the experimental data to verify the accuracy of the model and the acceptability of the convergence criterion.

The optimizer used in this study used a quasi-Newton approach based on the Broyden, Fletcher, Goldfarb, Shanno (BFGS) method for updating the inverse Hessian.[12] MATLAB® and the function *fminu* from the Optimization Toolbox[13] were used in this study to perform the error minimization. Note, however, that the specific routine is somewhat arbitrary in that any method able to minimize the scalar error function, ε^2, could be used.

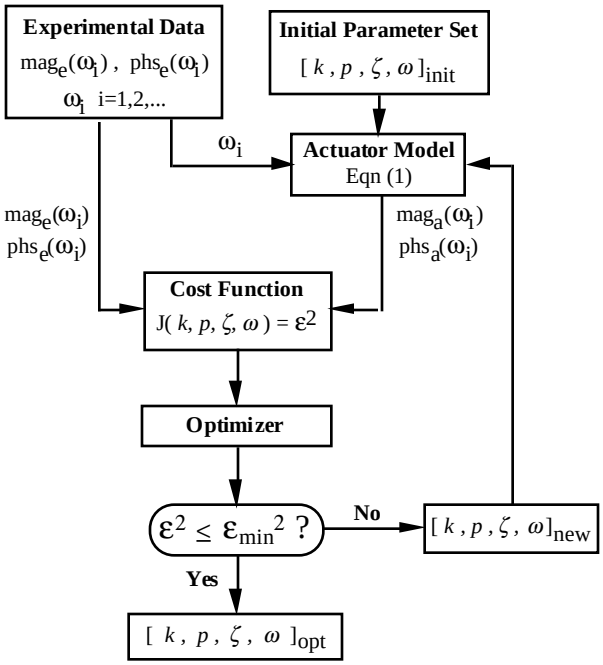

Figure 3 - Parameter estimation process.

The convergence criteria for the optimizer, $\varepsilon_{\min}^2$, the minimum allowable frequency response error, and $\frac{\Delta\theta}{\hat{\theta}}$, the change in the parameter values between successive iterations, were chosen to achieve qualitatively acceptable approximations to the experimental data. This was determined by plotting the experimental frequency response data and the frequency response associated with the estimated transfer function parameters on the same plot. The convergence criteria values were chosen small enough so that the frequency response error was judged to be acceptable but large enough so that convergence could be achieved.

The input-output frequency response error was judged to be acceptable when in the frequency range from 2 to 10 hertz the gain differences were less than about 0.1 and phase differences were less than about 3 degrees. These values represent approximately 10 percent of typical control system gain and phase margins. Errors greater than these could be acceptable if they appeared to be due to higher order effects (i.e., above third order) or nonlinearities in the experimental data.

The error function, ε^2, was formed in the following manner. The experimental and analytical frequency responses were represented in magnitude and phase form. The magnitude and phase values were stacked to form a vector as shown Eqn (2). Each element in the vectors corresponds to a particular frequency, ω_i, at which the experimental data was available.

$$\boldsymbol{y} = \begin{bmatrix} \boldsymbol{mag} \\ \boldsymbol{phs} \end{bmatrix} = \begin{bmatrix} mag(\omega_1) \\ mag(\omega_2) \\ mag(\omega_3) \\ \vdots \\ mag(\omega_n) \\ phs(\omega_1) \\ phs(\omega_2) \\ phs(\omega_3) \\ \vdots \\ phs(\omega_n) \end{bmatrix} \tag{2}$$

An error vector, $\boldsymbol{e}$, was then formed from the difference of the experimental and analytical frequency response data.

$$\boldsymbol{e} = \boldsymbol{y}_e - \mathbf{y}_a = \begin{bmatrix} \boldsymbol{mag}_e - \boldsymbol{mag}_a \\ \boldsymbol{phs}_e - \boldsymbol{phs}_a \end{bmatrix} = \begin{bmatrix} \Delta\boldsymbol{mag} \\ \Delta\boldsymbol{phs} \end{bmatrix} \tag{3}$$

where $\Delta\boldsymbol{mag}$ is the magnitude error and $\Delta\boldsymbol{phs}$ is the phase error. The weighted sum squared error, ε^2, was created by the weighted inner product of the error vector with itself.

$$\varepsilon^2 = \boldsymbol{e}^{\mathrm{T}}\boldsymbol{S}\boldsymbol{e} \tag{4}$$

where $\boldsymbol{S}$ is a diagonal matrix. The diagonal of $\boldsymbol{S}$ can be written

$$diag(\boldsymbol{S}) = \begin{bmatrix} c_m(\omega_1)\, c_m(\omega_2)\, c_m(\omega_3) \ldots c_m(\omega_n) \\ c_p(\omega_1)\, c_p(\omega_2)\, c_p(\omega_3) \ldots c_p(\omega_n) \end{bmatrix} \tag{5}$$

where $c_m(\omega_i)$ and $c_p(\omega_i)$ are arbitrary constants corresponding to the frequency ω_i, and n is equal to the number of frequency points in the experimental frequency response data set.

There are many ways to select the diagonal elements of the weighting matrix, $\boldsymbol{S}$, and a variety of error weighting schemes were studied. Emphasizing the penalty on phase error over the entire frequency range resulted in acceptable approximation to the experimental data. Accurate representation of the phase lag properties of the actuators is more important when applying the actuator models to control system analysis and design. In addition, by weighting phase error significantly more than magnitude error, magnitude variations in the frequency response data (due, for example, to amplitude dependent nonlinearities) played a lesser role in the parameter estimation process. Therefore, more heavily penalizing the phase error resulted in models that more closely approximate the key dynamics of the actuators.

Application of Parameter Estimation Procedure

The parameter estimation procedure was applied to construct actuator models for the BACT wind-tunnel model using the available experimental frequency response data. The weighting strategy described above was used with $c_m(\omega_i)$, $i=1,2,3,...,n$ equal to one and the values of $c_p(\omega_i)$, $i=1,2,3,...,n$ equal to ten. The value for the convergence criteria that resulted in acceptable convergence was $\varepsilon^2_{\min}$ = 1e-04, and $\frac{\Delta\theta}{\hat{\theta}}$ = 1e-04, the default values for *fminu*.

The estimation process was initiated with a variety of initial guesses for the unknown parameter set, k, p, ω, ζ. For cases in which there was no aerodynamic loading, the initial guess played a relatively small role in convergence. For cases in which aerodynamic load was present, however, the solution was more sensitive to the initial parameter set and more iterations were generally required for convergence. The most critical initial parameter value was the second order frequency, ω. Several initial guesses were sometimes required to achieve convergence.

Slower convergence for the aerodynamically loaded conditions can be attributed to the nature of the experimental data. Wind-tunnel turbulence resulted in lower signal-to-noise ratios and consequently more noise in the frequency response data than when no turbulence was present. Aerodynamic load may also contribute to nonlinearities or higher order effects that cannot be approximated well with the third order actuator model in Eqn (1). Nonlinearities, higher order effects, and noise in the experimental frequency response data result in larger weighted sum squared frequency response error.

In addition, the sensitivity to the initial guesses for the parameters indicates the possibility of local minima or very flat solution spaces. This problem was addressed by using multiple initial guesses and evaluating the convergence patterns and the similarity of the converged parameter sets. The sensitivity of the converged solutions under load indicates that, while similar accuracy can be achieved over the range of frequencies of interest, the resulting bandwidth and resonant peak properties of the actuators (i.e., the values of p, ω, and ζ) can vary significantly. However, since no experimental data was available near the bandwidth frequencies the accuracy of the estimates of p, ω, and ζ in terms of bandwidth and resonant peaks could not be addressed in this study.

The parameter sets identified from the experimental data are shown in Tables 1 and 2. Note that the parameters k and p did not vary nearly as much over time and aerodynamic loading condition as did ω and ζ. Frequency response data created from the analytical models using the parameters in Tables 1 and 2 very closely approximate the experimental data with respect to both magnitude and phase over the frequency range from 0.5 to 12 Hertz (at which experimental data was available). Figure 4 shows a comparison of the frequency responses of the experimental and analytical data for a typical case.

Note that the first order lag, p, remained very large for both loaded and unloaded conditions throughout the test. As a result, the term $\frac{p}{s+p}$ is almost unity over the range of frequencies of interest for the BACT and its contribution to the frequency responses based on the transfer function model in Eqn (1) is negligible. Therefore, the actuator model is in a sense over-parameterized and a second order transfer function of the following form could also be used with equivalent results.

$$\frac{\delta(s)}{\delta_c(s)} = \frac{k\omega^2}{s^2 + 2\zeta\omega s + \omega^2} \tag{6}$$

Table 1 - Analytical transfer function parameters with no aerodynamic load.

Control Surface	*Test Stage*	*k (deg/deg)*	*p (1/sec)*	*ω (rad/sec)*	*ζ*
Trailing	Early	1.0198	10000	165.26	0.5624
Edge	Middle	1.0413	10000	223.57	0.7269
Actuator	Late	1.0159	10000	212.50	0.5776
Upper	Early	1.1617	10000	164.00	0.8478
Spoiler	Middle	1.1180	10000	142.02	0.6463
Actuator	Late	1.1219	10000	138.21	0.6024
Lower	Early	1.0903	10000	168.45	0.7583
Spoiler	Middle	1.0362	10000	155.08	0.6795
Actuator	Late	1.0942	10000	175.77	0.7885

Table 2 - Analytical transfer function parameters with aerodynamic load.

Control Surface	*Test Stage*	*k (deg/deg)*	*p (1/sec)*	*ω (rad/sec)*	*ζ*
Trailing	Early	0.9607	10000	139.20	0.4281
Edge	Middle	0.9345	10000	133.44	0.4055
Actuator	Late	1.0468	6898	242.32	0.7475
Upper	Early	1.1152	9995	125.65	0.6187
Spoiler	Middle	1.1702	9996	135.87	0.6827
Actuator	Late	1.0767	2.97e08	100.72	0.4615
Lower	Early	1.0289	9998	145.07	0.6314
Spoiler	Middle	1.0265	9999	150.85	0.6444
Actuator	Late	N/A	N/A	N/A	N/A

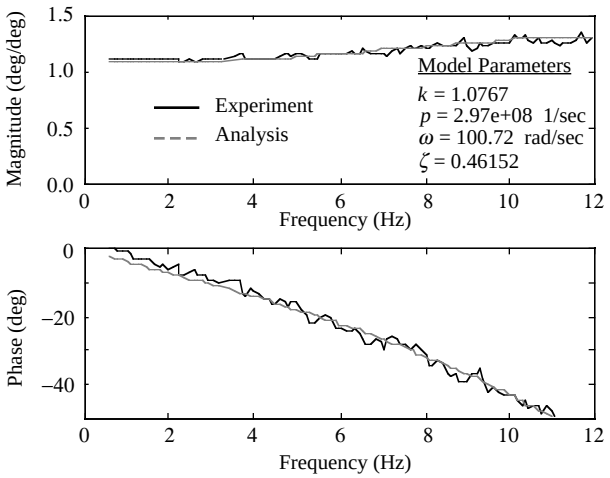

Figure 4 - Frequency response comparison - upper spoiler with aerodynamic load (M=0.80, q=140 psf), late in the wind-tunnel test.

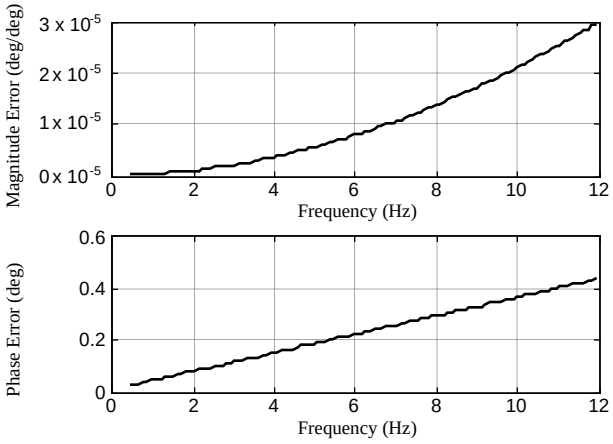

Figure 5 - Frequency response error between third and second order models of the lower spoiler, no aerodynamic load (M=0, q=0 psf), early in the wind-tunnel test.

Figure 5 shows the magnitude and phase differences between the frequency responses of the third and second order actuator models, Eqns (1) and (6), respectively for a typical case. The errors in both magnitude and phase are very small and clearly justify the use of the second order transfer function form, Eqn (6).

Despite the over-parameterization and convergence issues, the parameter estimation process was successful in constructing analytical models of the actuators. Therefore, the actuator models presented in Eqns (1) and (6) with the parameter values presented in Tables 1 and 2 can be effectively utilized to characterize the dynamic behavior of the BACT actuators.

Analysis of BACT Actuator Behavior

Using the analytical actuator models obtained during the parameter identification process, an analysis was done to determine consistency of the actuator dynamics during the BACT wind-tunnel test. Two issues of primary concern were addressed -- the effect of variations over time (i.e., servo gain variations and mechanical wear) and the effect of hinge moments on the dynamic characteristics of the actuators. Variations over time were considered by comparing data over the three test stages (Early, Middle, and Late). Hinge load effects were considered by comparing data for the loaded and unloaded conditions.

If the input-output frequency response behavior of the actuators change significantly over time and/or with hinge loads it would be important to consider these effects in the design of control laws to assure that stability and performance is maintained. Significant variations in this study were based on 10 percent of the typical gain and phase margins mentioned previously, that is, magnitude variations of more that 0.1 and phase variations of more than 3 degrees.

The results of comparing the data among the three test stages indicate notable differences in the parameters ω and ζ due to variations over time as can be seen by comparing the data presented in Tables 1 and 2. Figures 7 and 8 indicate how actuator frequency and damping parameters varied over time with no aerodynamic hinge load. The effect of the parameter variations is primarily to introduce phase variations in the actuator frequency response as shown in Figure 9 which depicts a chronological comparison of the trailing edge actuator frequency responses for the unloaded condition (M=q=0) and is representative of the effects of time variations.

The differences in the phase response over the 0.5 - 12 hertz frequency range become significant at

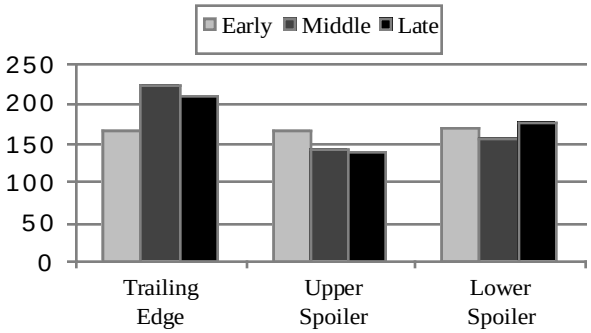

Figure 7 - Frequency parameter, ω, - unloaded conditions, throughout the wind-tunnel test.

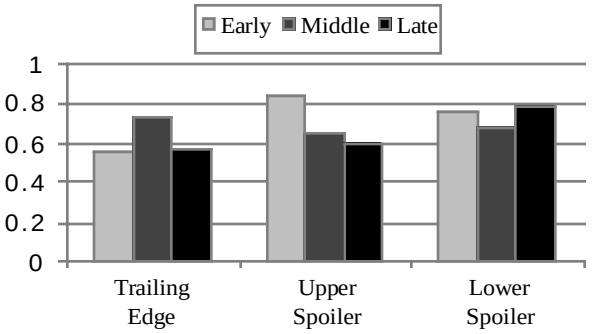

Figure 8 - Damping parameter, ζ, - unloaded conditions, throughout the wind-tunnel test.

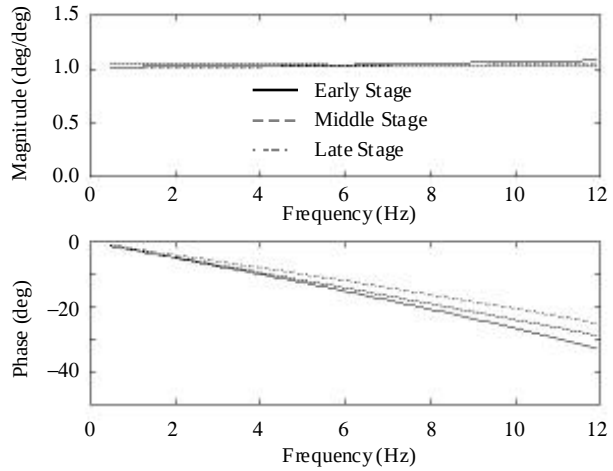

Figure 9 - Effects of servo gain variations and mechanical wear for trailing edge frequency response with no aerodynamic load.

frequencies beyond 6 Hertz. The key aeroelastic frequencies for the BACT wind-tunnel model are in the range from 3 to 5 hertz. The smaller variations in phase at these frequencies are generally within the allowable range. However, the variations over time could become significant if phase uncertainty beyond 5 hertz was an issue in the control system design.

The effect of hinge moments on actuator behavior are less significant. Figures 10 and 11 indicate how actuator frequency and damping parameters varied due to aerodynamic load early in the test. Note that the loaded conditions correspond to a range of Mach numbers and dynamic pressures and so characterize the qualitative effects of hinge load. Despite the differences in the actuator parameters due to aerodynamic loading the influence of hinge load had no significant impact on any of the actuator frequency responses in the frequency range of interest (0.5 to 12 Hertz), as shown in Figure 12.

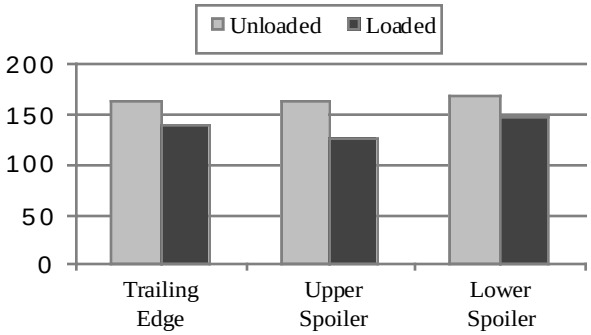

Figure 10 - Frequency parameter, ω, - unloaded and loaded conditions, early in the wind-tunnel test.

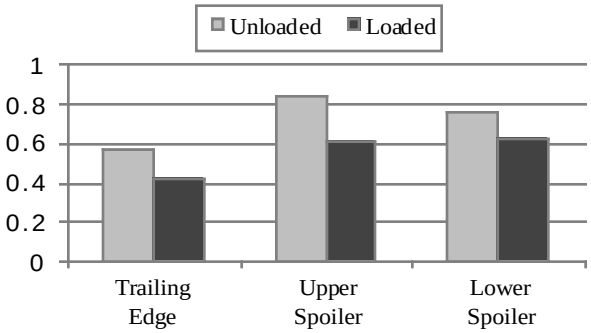

Figure 11 - Damping parameter, ζ, - unloaded and loaded conditions, early in the wind-tunnel test.

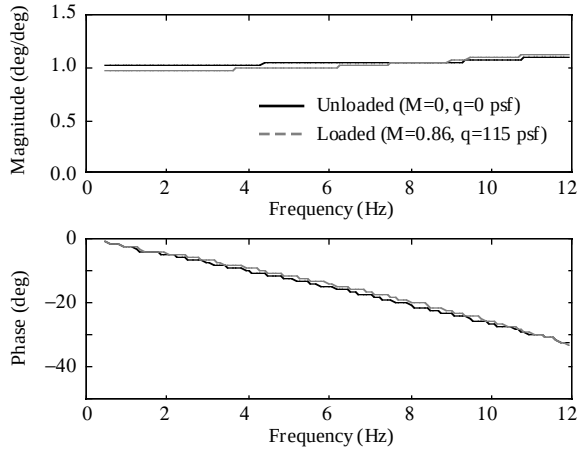

Figure 12 - Effect of aerodynamic load - trailing edge frequency response, early in the wind-tunnel test.

Note that the comparisons at the early stage of the test are effectively isolated from wear and gain variations since little wear and no gain changes had yet occurred. This is not the case for the middle and late stages of the test. Therefore, comparisons between the loaded and unloaded parameter estimates at the middle and late stages combine all the possible effects.

The actuator frequency responses, as a whole, varied little over time and under aerodynamic load throughout the wind-tunnel test. This would imply that very simple actuator models could be used in the analysis, design, and simulation of control systems for the BACT wind-tunnel model. The actuators can be effectively modeled by constant coefficient, second order transfer functions of the form shown in Eqn (6). The coefficients do not, in general, have to be scheduled with hinge load but some scheduling for wear state might be required if small phase variations are an issue in control system design. In addition, the parameter variations presented in Tables 1 and 2 could be used to quantify typical actuator uncertainties for application to robustness studies of BACT controllers.

Concluding Remarks

Experimental actuator frequency response data, generated during an experiment involving the Benchmark Active Control Technology (BACT) wind-tunnel model in the Langley Transonic Dynamics Tunnel, was used as a basis for estimation of parameters in transfer function models of the BACT actuators. A parameter estimation approach based on minimizing the difference between experimental and model-based frequency responses was successfully employed to model the dynamic characteristics of the actuators of the BACT wind-tunnel model using third order, constant coefficient transfer functions. It was also determined that the actuator model could be reduced to second order with negligible impact on the frequency response properties over the frequency range for which experimental data was available.

Model-based frequency response data closely approximated the experimental data over a wide range of wind-tunnel operating conditions. Comparative analysis of the analytical data corresponding to various test conditions also indicated little change in actuator frequency response behavior due to mechanical wear, servo gain variations, and aerodynamic load. As a result, the transfer function models developed herein can be used to model the dynamics of the BACT actuators over a wide range of wind-tunnel operating conditions for application to control system design and analysis. In addition, the parameter variations associated with mechanical wear, servo gain variations, and aerodynamic loading effects can be used to develop uncertainty models of the actuators for application to robustness analysis of BACT controllers.

Acknowledgments

The authors wish to acknowledge Sherwood Hoadley, Robert Scott, Carol Wieseman, and Michael Sorokach for their significant assistance.

References

[1] Durham, M.H.; Keller, D.F.; Bennett, R.M.; and Wieseman, C.D.: A Status Report on a Model for Benchmark Active Controls Testing. AIAA Paper No. 91-1011.

[2] Waszak, M.R.: *Modeling the Benchmark Active Control Technology Wind-Tunnel Model for Application to Flutter Suppression*. AIAA Paper No. 96-3437. Presented at the AIAA Atmospheric Flight Mechanics Conference. San Diego, CA. July 29-31, 1996.

[3] Hardin, J.C.: *Introduction to Time Series Analysis*. NASA RP-1145, pp. 75-81. Second Printing November 1990.

[4] Bennett. R.M.; Eckstrom, C.V.; Rivera, Jr., J.A.; Dansberry, B.E.; Farmer, M.G.; and Durham, M.H.: The Benchmark Aeroelastic Models Program - Description and Highlights of Initial Results. NASA TM-104180, December 1991.

[5] Rivera, Jr., J.A.; Dansberry, B.E.; Bennett, R.M.; Durham, M.H.; and Silva, W.A.: NACA 0012 Benchmark Model Experimental Flutter Results with Unsteady Pressure Distributions. AIAA Paper No. 92-2396. Proceedings of the 33rd AIAA/ASME/ASCE/AHS/ASC Structures, Structural Dynamics, and Materials Conference. Dallas, TX, April 1992.

[6] Rivera, Jr., J.A.; Dansberry, B.E.; Durham, M.H.; Bennett, R.M.; and Silva, W.A.: Pressure Measurements on a Rectangular Wing with a NACA 0012 Airfoil During Conventional Flutter. NASA TM-104211, July 1992.

[7] Baals, D.D. and Corliss, W.R.: Wind Tunnels of NASA. pp. 79-81. NASA SP-440.

[8] Sorokach, M. R., Jr.: *Miniature Linear-To-Rotary Motion Actuator*. NASA CP 3205, May 1993.

[9] Wieseman, C.D.; Hoadley, S.T.; and McGraw, S.M.: On-Line Analysis Capabilities Developed to Support Active Flexible Wing Wind-Tunnel Model. *Journal of Aircraft*. Volume 23, Number 1. pp. 39-44. January-February 1995.

[10] Truxal, J. G., ed.: *Control Engineers' Handbook*. McGraw-Hill Book Company, Inc., 1958. Section 15.

[11] Buttrill, C.S.; Bacon, B.J.; Heeg, J.; Houk, J.A.; and Wood, D.V.: *Aeroservoelastic Simulation of an Active Flexible Wing Wind Tunnel Model*. NASA TP-35100, p. 9, April 1996.
[12] Gill, P.E.; Murray, W.; and Wright, M.H.: *Practical Optimization*. Academic Press, New York; London. 1981.
[13] Grace, A.: *Optimization Toolbox, For Use with Matlab*. The MathWorks, Inc., 1992.